

# Pathogenesis of Experimental Lipid Keratopathy

## *An Ultrastructural Study of an Animal Model System*

Sanford I. Roth,\* E. Lee Stock,† Janet M. Siel,† Alan Mendelsohn,† Chittaranjan Reddy,†  
David G. Preskill,† and Santibrata Ghosh‡

**The histology and ultrastructure of experimental lipid keratopathy were studied in hypercholesterolemic rabbits in which the insertion of corneal sutures induced vascularization and subsequent lipid deposition in the anterior stroma. Lipid accumulated in the keratocytes, the pericytes and occasionally in the endothelial cells of the capillaries. The lipid-laden keratocytes were concentrated in the region of the capillaries. No lipid was seen in the control rabbits. In the hypercholesterolemic rabbit with sutures, intracellular lipid in the keratocytes was present largely in nonmembrane-limited droplets with smaller amounts of membrane-limited cholesterol crystals and rare numbers of myelin figures. In addition, large, lipid-engorged spherical cells were present. The numerous phagolysosomes seen ultrastructurally suggest that some of these cells probably represent macrophages. Keratocytes and the large, spherical lipid-engorged cells show focal degenerative changes, including pyknotic nuclei, cytoplasmic coagulation and membrane loss, leaving extracellular mixed accumulations of lipid and cytoplasmic organelles. Small numbers of lymphocytes and plasmacytoid cells were present. No corneal lipid was seen in animals with normocholesterolemia, with or without sutures. In hypercholesterolemic animals, a few lipid-laden keratocytes without macrophages were identified even in the absence of vessels. These morphologic studies support the hypothesis that the accumulation of the corneal lipid in this animal model of lipid keratopathy is the result of increased lysosomal uptake of lipid, probably as low density lipoprotein, from the extracellular space by the keratocytes. The rate of metabolism of this lipid is insufficient to clear the cells of the lipid and the subsequent lipid inspissation results in keratocyte death, leading to macrophage accumulation of lipid and free lipid in the stroma. Invest Ophthalmol Vis Sci 29:1544–1551, 1988**

Human lipid keratopathy is characterized by the accumulation of lipid in the stroma of the cornea.<sup>1</sup> There is both a primary form with no known antecedent event, and a secondary variety, associated with corneal vascularization, and occurring following infection,<sup>2</sup> trauma<sup>3</sup> or contact lens wear.<sup>4</sup> Clinically, yellowish-white opacities develop in the cornea in the vicinity of the neovasculature. The degree of visual

loss depends upon the location and density of lipid deposition. Since the definitive description of lipid keratopathy by Cogan and Kuwabara in 1958,<sup>1</sup> corneal lipid deposition has been studied in experimental rabbit eyes<sup>5-7</sup> and in human specimens.<sup>8</sup> When rabbits are maintained on a high cholesterol diet, the intrastromal placement of 8-0 silk sutures induces corneal vascularization and within 2 weeks a gradual intracorneal deposition of lipid occurs near the newly formed capillaries.<sup>6</sup> The fully developed disease in the rabbit grossly resembles the secondary lipid keratopathy present in humans. The traditional pathologic description of the human lipid keratopathy has included "lipid-laden macrophages"<sup>3</sup> and intracellular and extracellular lipid.<sup>1</sup> This paper presents the results of a histologic and ultrastructural study of the fully developed lipid keratopathy in our rabbit model system.

### Materials and Methods

The experimental procedure producing lipid keratopathy in the rabbit has been described in detail.<sup>6,7</sup> The control diet consisted of vegetarian rabbit chow

---

From the Departments of \*Pathology and †Ophthalmology, and the ‡Program in Biochemistry, Northwestern University Medical School, and the †Department of Ophthalmology, Veterans Administration Lakeside Medical Center, Chicago, Illinois.

Presented in part at the annual meeting of the United States and Canadian Academy of Pathology (United States-Canadian Division of the International Academy of Pathology), Washington, DC, February 28–March 4, 1988 (Lab Invest 58:79A, 1988).

Supported in part by an unrestricted grant to the Department of Ophthalmology by Research to Prevent Blindness, Inc., and the Veterans Administration Research Service (176 34 3874-01).

Submitted for publication: November 20, 1986; accepted April 20, 1988.

Reprint requests: Sanford I. Roth, MD, Department of Pathology, Northwestern University Medical School, 303 E. Chicago Avenue, Chicago, IL 60611.

**Table 1.** Designation of experimental and control groups

Group	Diet	Sutures
I Experimental	0.5% chol. (dissolved in oil)	Yes
II Control	0.5% chol. (dissolved in oil)	No
III Control	Normal	Yes
IV Control	Normal	No

(Purina Rabbit Chow, Checkerboard Square, St. Louis, MO), *ad libidum*. A high cholesterol stock was prepared by dissolving 5 g of cholesterol in 50 g of partially hydrogenated soybean oil (Wesson Oil) at 50°C. This cholesterol stock was mixed with 1 kg of the vegetarian rabbit chow to give a concentration of 0.47% cholesterol (w/w). Animals on a high cholesterol diet were given 100 g of the high cholesterol chow per day, followed by vegetarian chow *ad libidum*. Four groups of rabbits, three control and one experimental (Table 1) were used. Corneal sutures were placed in animals of groups I and III, 8 days after animals of groups I and II began a high cholesterol diet. Animals were sacrificed by intramuscular ketamine hydrochloride, xylazine hydrochloride and intracardiac pentobarbital at 15 weeks, the time when all of the experimental animals exhibited suture-induced vascularization and visible lipid deposits in the hypercholesterolemic rabbits (stage 3).<sup>6,7</sup> All animals were maintained and used in conformance with the ARVO Resolution on the Use of Animals in Research.

Corneas were removed from rabbit eyes and immediately placed in plastic Petri dishes containing Balanced Salt Solution. Under an operating microscope ( $\times 40$  magnification), lipid-containing corneal quadrants were excised with a razor blade. Each was bisected through the densest area of visible lipid deposit. One half was frozen, unfixed in OCT with liquid nitrogen. Five micron sections were cut at  $-20^{\circ}\text{C}$  on a cryostat, melted on to ovalbumin pretreated glass slides and stained with either toluidine blue or oil red O. The remaining half of each opaque quadrant was cut into  $2 \times 2$  mm sections, fixed at  $4^{\circ}\text{C}$  for 2 hr in Karnovsky's paraformaldehyde-glutaraldehyde<sup>9</sup> in sodium cacodylate buffer, pH 7.4, and subsequently stored at  $4^{\circ}\text{C}$  in 0.1 N sodium cacodylate buffer. The tissue was postfixated in 1% osmium tetroxide in phosphate buffer, pH 7.4, for 1 hr at room temperature, followed by 10 min in lactated Ringer's solution, pH 7.3, dehydrated in graded alcohols and embedded in epon. One (1) micron sections were cut with a glass knife on an LKB Ultratome III (Bromma, Sweden) and stained with 1% toluidine blue. Seventy (70) to 100 nm sections were cut with a diamond

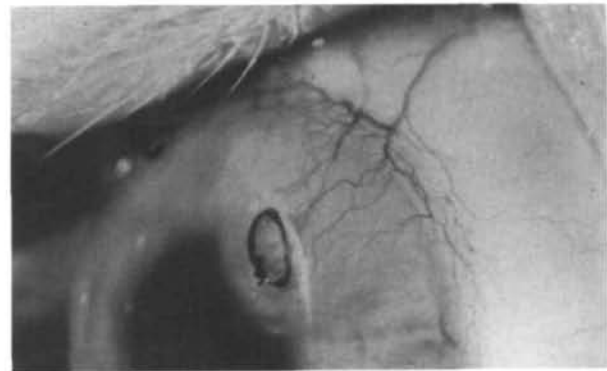


**Fig. 1.** Slit-lamp photograph of a sutured eye (O.D.) of a Group I rabbit 29 days after suture implantation, with a large area of corneal lipid accumulation surrounding the suture. A clear region is present between the limbus and the area of lipid. The vascularization of the region is prominent.

knife on an LKB Ultratome III, and placed on copper-rhodium 200 mesh grids. After 1 hr in 7% uranyl acetate in distilled water and a distilled water rinse, grids were stained with lead citrate<sup>10,11</sup> and uranyl acetate. Grids were then examined with Philips 301 electron microscope (Eindhoven, The Netherlands) at 80 kV.

## Results

### Gross Morphology

The progressive vascularization and lipid accumulation in rabbit eyes of the of group I animals of the model were previously described in detail.<sup>6,7</sup> Blood vessels grow toward the sutures at a constant rate of

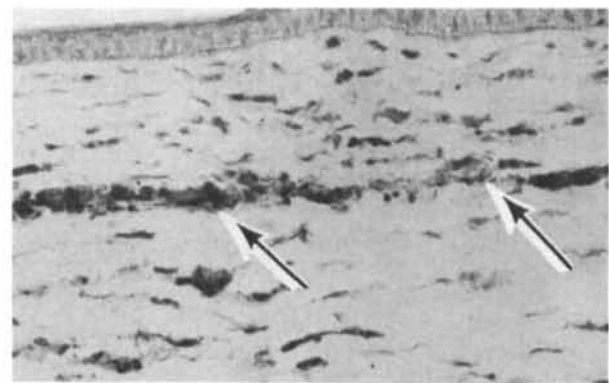


**Fig. 2.** Light micrograph of the cornea demonstrating abundant oil red O positive droplets (arrows) in spindle-shaped keratocytes and spherical macrophages in the subepithelial region. Group I. Oil red O with hematoxylin,  $\times 143$ .

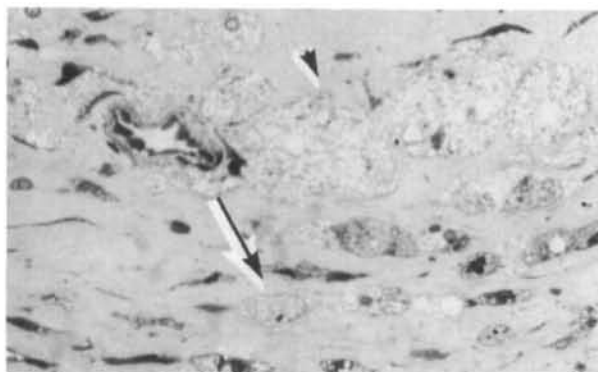


**Fig. 3.** Light micrograph of a 1  $\mu\text{m}$  section demonstrating individual lipid droplets in the cytoplasm of spindle-shaped keratocytes (arrow) and large spherical macrophages (arrowhead). The latter are concentrated near a capillary. Group I. Toluidine blue,  $\times 350$ .

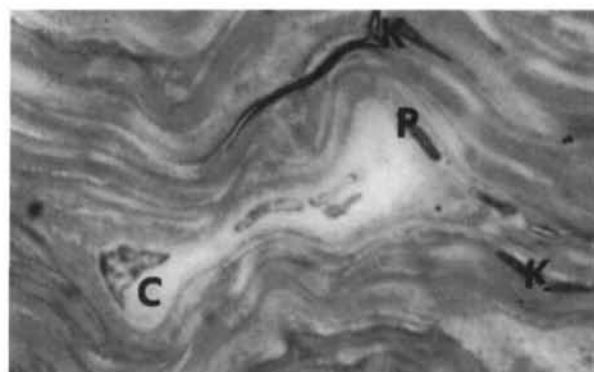


**Fig. 4.** Light micrograph of a 1  $\mu\text{m}$  section of a cornea of a control animal (no cholesterol, sutures) revealing a normal epithelium and stroma. No lipid deposition is seen in the stroma, keratocytes (K), capillary (C), or pericytes (P). Toluidine blue. Group III,  $\times 1410$ .

0.24 mm/day, exhibiting straight to moderately sinuous courses. The earliest grossly visible lipid deposits appear within 12 days of suture implantation as a somewhat granular, cloudy area near the tips of the blood vessels. These deposits gradually increase in

size and opacity, achieving maximum density near the sutures, 25 days following suture placement, when all animals have some lipid. A clear zone of cornea typically remains between the limbus and base of the opaque arc (Fig. 1). As previously re-



**Fig. 5.** Electron micrograph of the corneal stroma with stromal keratocytes containing variable numbers of lipid droplets (L). Myelin figures (arrow) are present in some keratocytes. Uranyl acetate and lead citrate. Group I,  $\times 3900$ .

**Fig. 6.** Electron micrograph of the corneal stroma. The keratocytes contain variable numbers of lipid droplets (L). The keratocytes nearer the capillary (top of micrograph) generally have larger numbers of droplets in their cytoplasm. Some active keratocytes with abundant parallel arrays of granular endoplasmic reticulum are free of lipid droplets. Uranyl acetate and lead citrate. Group I,  $\times 3650$ .



ported,<sup>6</sup> there is no grossly visible lipid in animals of groups II, III, or IV.

#### Light Microscopy

In group I animals, large quantities of lipid are present between the lamellae of the anterior corneal stroma in all of the experimental animals, though the amount of lipid is variable from 2+ to 4+. These accumulations of lipid always occur in association

with cell nuclei, either as small droplets in otherwise normal keratocytes or in large accumulations (Fig. 2). One (1) micron sections demonstrate a hypercellular stroma containing the normally elongated, thin, stromal fibroblasts with slender processes extending between collagen lamellae. Some of these fibroblasts, otherwise normal in location and morphology, contain lipid droplets (Fig. 3). Large, spherical cells, filled with lipid are present, often in the region of the keratocytes (Fig. 3). Group II, III and IV animals have no

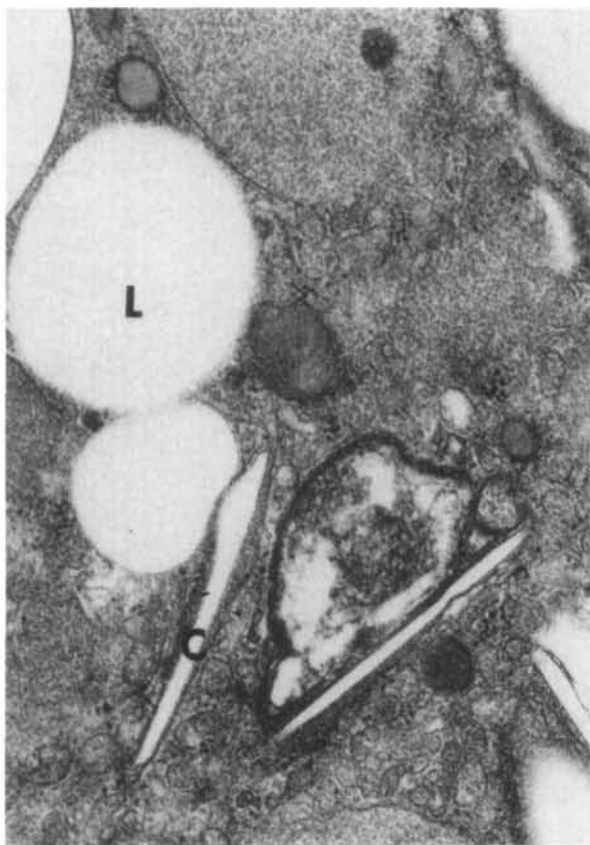


Fig. 7. Electron micrograph of a keratocyte showing the non-membrane-limited lipid droplets (L) and membrane-limited cholesterol clefts (C) with surrounding electron-dense material. Uranyl acetate and lead citrate. Group I,  $\times 41,100$ .

lipid-containing keratocytes or macrophages (Fig. 4). Capillaries are seen in the region of the sutures in group III animals (Fig. 4).

### Electron Microscopy

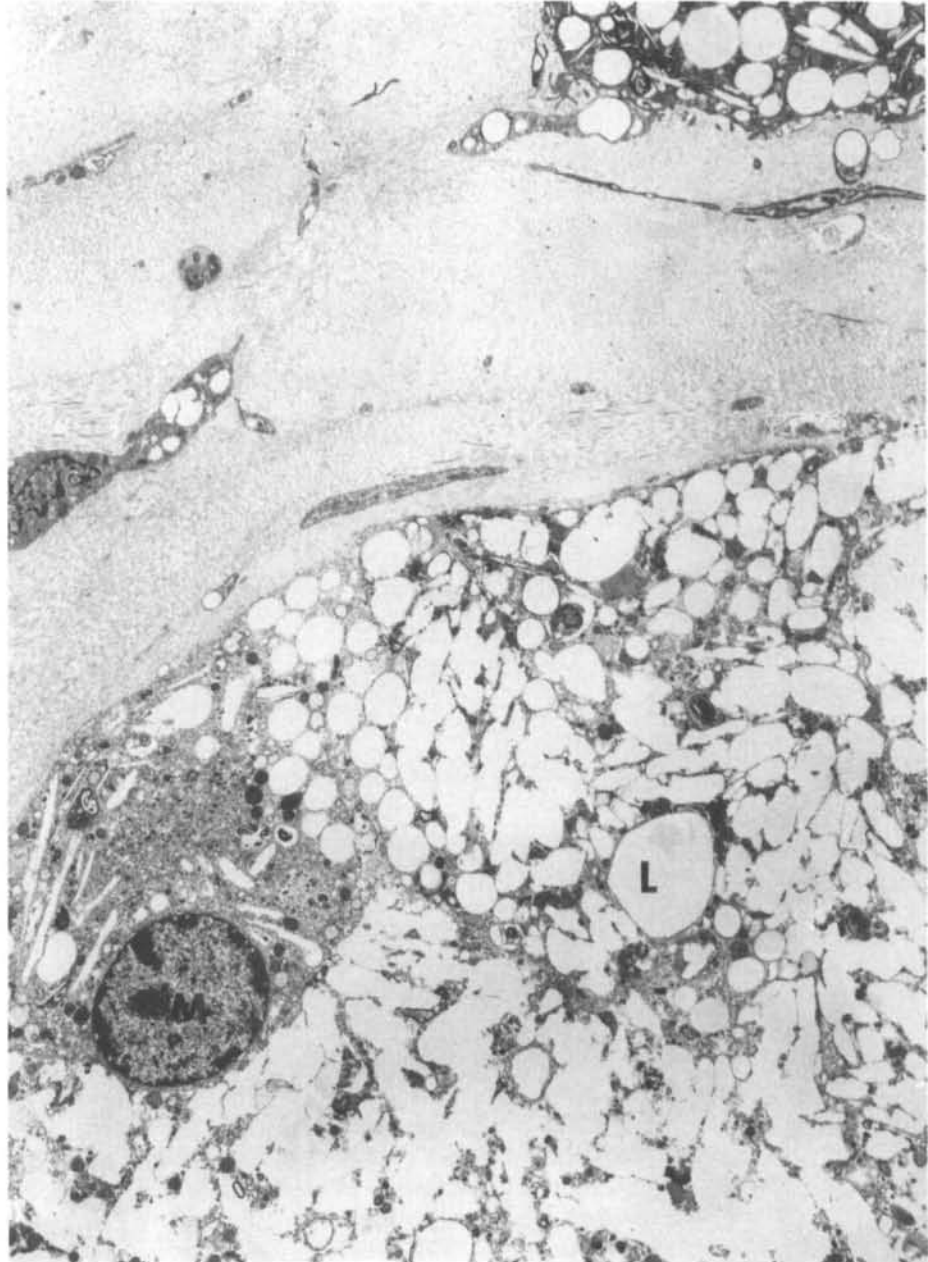
The epithelium, Bowman's layer, endothelium and Descemet's membrane are within normal limits, without lipid, in all groups. There is a spectrum of keratocyte pathology in the group I animals. Normal keratocytes with varying degrees of granular endoplasmic reticulum are present between collagen lamellae. Keratocyte nuclei are spindle-shaped and irregular with marginated chromatin and no nucleoli. Many otherwise normal keratocytes contain sparse, nonmembrane-limited lipid droplets in the cell cytoplasm and dendrites (Fig. 5). Other keratocytes and their dendritic processes show increasing degrees of engorgement by non-membrane limited lipid drop-

lets (Fig. 6), membrane-limited cholesterol crystals (Figs. 5, 7). Also present are degenerating keratocytes with pyknotic nuclei and myelin figures. Lipid-filled phagolysosomes are rare in clearly identifiable keratocytes. Intracytoplasmic needle-shaped cholesterol crystals are membrane-limited and often surrounded by an area of increased electron density (Fig. 7). Neither the lipid droplets nor cholesterol crystals exhibit any obvious relationship to other cell organelles. Usually in the vicinity of lipid-laden keratocytes showing degeneration are extremely large, spherical, lipid-containing cells which contain less rough endoplasmic reticulum, many cytoplasmic inclusion bodies of varying electron density, phagolysosomes, cholesterol clefts,<sup>12</sup> numerous small pseudopod-like cytoplasmic extensions, and spherical nuclei often with prominent nucleoli (Fig. 8). The nuclear chromatin is lightly marginated. These cells usually surround or are in close relationship to obvious lipid-laden keratocytes, and are most prominent near the blood vessels. In some areas the lipid droplets are intermixed with cholesterol clefts,<sup>12</sup> and interspersed with intact cell organelles and cytosolic debris with incomplete cell membrane fragments. In other areas, the cell membranes could no longer be identified, though degenerating cell organelles, cytosolic debris and myelin figures are present amid the lipid (Fig. 9). All apparently extracellular lipid observed is associated with cell debris. The endothelial cells of the capillaries contain numerous pinocytotic vesicles and luminal microvilli. Some endothelial cells of the capillaries and their pericytes contain lipid droplets (Fig. 10). A few plasma cells and lymphocytes, located between the collagen lamellae, contribute to the cellularity of the stroma, but do not contain lipid droplets. The keratocytes of the control (groups II, III and IV) animals are within normal limits. No lipid is seen in the keratocytes or stroma, and there are no lipid-laden macrophages. Capillaries and pericytes, also without lipid, are seen in group III animals.

### Discussion

A diffuse circumferential infiltration of lipid, resembling the human arcus senilis, was produced in the cornea of hypercholesterolemic rabbits by Rodger.<sup>5</sup> Incision of the cornea, followed by suturing, greatly accelerated and altered the distribution of the lipid deposition. The lipid in the latter situation was near the injury. Stock et al<sup>16,7</sup> produced a localized lipid keratopathy, closely resembling human secondary lipid keratopathy, by inserting a suture without

**Fig. 8.** Electron micrograph of macrophage (M) with a spherical nucleus, abundant lipid droplets (L) and cholesterol clefts. Spindle-shaped keratocytes with lipid droplets are also seen in the stroma. Uranyl acetate and lead citrate. Group 1,  $\times 3600$ .



an incision into the corneas of hypercholesterolemic rabbits.

Our ultrastructural studies on this model have shown a large number of the lipid-containing cells to be keratocytes. The lipid in these keratocytes largely consists of nonmembrane-limited lipid droplets, probably cholesterol esters,<sup>13</sup> lesser numbers of cholesterol clefts and rare myelin figures. The initial uptake and subsequent metabolism of cholesterol in the

keratocyte is presumably similar to that in the fibroblast<sup>14</sup>: ie, internalization of the serum low density lipoproteins (LDL) by membrane-limited endosomes with subsequent transfer to lysosomes, the metabolism of the LDL and proteins into free cholesterol and fatty acids by the lysosomal lipases and esterases, and the hydrolysis of the proteins into amino acids, which along with the fatty acids are used by appropriate cell metabolic cycles. The cholesterol is then re-esterified

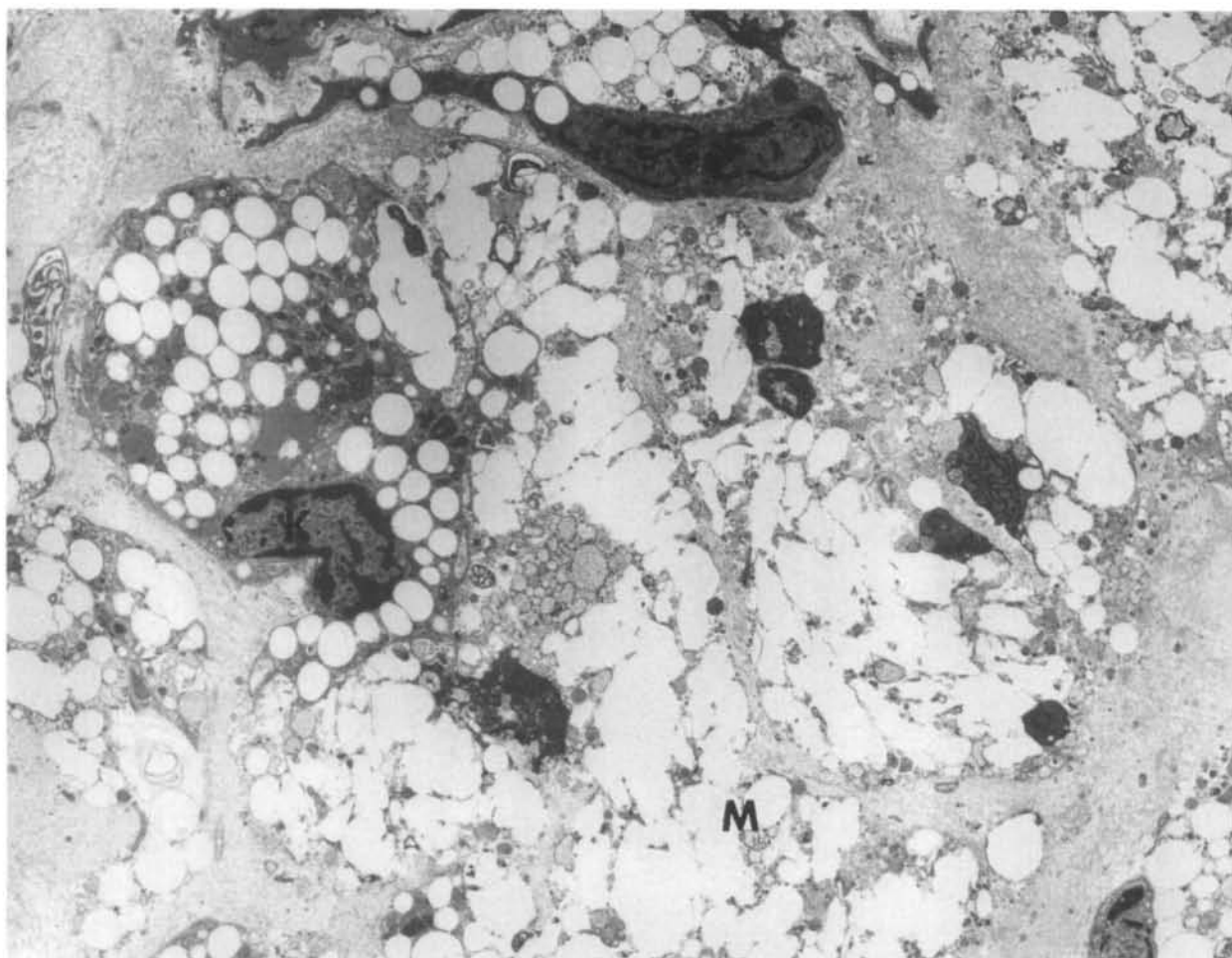


Fig. 9. Electron micrograph of keratocytes (K) with lipid droplets surrounded by necrotic macrophage-like cells (M) with degenerating nuclei and coalescing lipid droplets. Uranyl acetate and lead citrate. Group I,  $\times 3900$ .

in the Golgi region for use in membrane metabolism or transferred to the cytoplasm for storage in non-membrane-limited droplets, as we see in the keratocytes in the current study. This does not preclude the possibility that unprocessed cholesterol esters are present in such droplets in abnormal or exacerbating situations, as described by Basu et al.<sup>14</sup> Thus we postulate that the rate-limiting step in the metabolism and excretion of the cholesterol by the keratocytes in the presence of hypercholesterolemia is in the final step, ie, elimination of cholesterol esters from the cytoplasm. The keratocytes become engorged with lipid and undergo apoptosis, and the macrophages phagocytose the remaining cell debris, including the lipid droplets, but in other situations leave the lipid free in the stroma. In the classic description of lipid keratopathy, the lipid-laden cells are described as macrophages, and they have been compared to the macro-

phages seen in atherosclerotic plaques<sup>15</sup> in which foam cells constitute one of the major cells. Recent evidence has suggested that in atherosclerosis the smooth muscle cell may also develop into foam cells and subsequently the atherosclerotic plaque.<sup>15</sup> Because of the nuclear and other structural differences, we feel that some cells are macrophages, but it would appear that these are usually associated with keratocyte necrosis. This is consistent with the observations of Rodger.<sup>5</sup> In other areas with necrotic cells, macrophages would remove only the cellular debris, leaving the free stromal lipid, seen in long-standing human cases of lipid keratopathy (Roth and Stock, unpublished data).<sup>8</sup>

In summary, it is our hypothesis that experimental lipid keratopathy begins as an increased intracellular uptake of LDL and cholesterol esters, primarily in the stromal keratocytes with lesser amounts in the peri-



**Fig. 10.** Electron micrograph of a pericyte containing numerous nonmembrane-limited lipid droplets (L). One droplet contains a myelin figure (arrow). Uranyl acetate and lead citrate. Group I,  $\times 8558$ .

cytes and endothelial cells. As the intracellular lipid metabolic mechanisms of the keratocytes are overwhelmed, cell death occurs and the lipid and proteinaceous cell debris is liberated into the corneal stroma. This debris is phagocytosed by macrophages. It is probable that the process in man as in the rabbit is related to the altered lipid metabolism associated with the hyperlipidemia and hypercholesterolemia.<sup>12</sup> The process may be reversible until keratocyte death occurs.

**Key words:** lipid keratopathy, cornea, vascularization, ultrastructure, hypercholesterolemia

### Acknowledgment

The technical assistance of Ms. Susan Boyle-Vavra is greatly appreciated.

### References

1. Cogan DG and Kuwabara T: Lipid keratopathy and atheroma. *Trans Am Ophthalmol Soc* 56:109, 1958.
2. Marsh RJ and Marshall J: Treatment of lipid keratopathy with the argon laser. *Br J Ophthalmol* 66:127, 1982.
3. Garner A and Klintworth GK: *Pathobiology of Ocular Disease*. New York, Marcel Dekker, Inc., 1982, pp. 1445-1451.
4. Brightbill FS, Lange RH, and Stevens TS: Lipid keratopathy associated with aphakic contact lens wear. Poster Presentation at the American Academy of Ophthalmology Annual Meeting Chicago, Illinois, November, 1983.
5. Rodger FC: A study of the ultrastructure and cytochemistry of lipid accumulation and clearance in cholesterol-fed rabbit cornea. *Exp Eye Res* 12:88, 1971.
6. Stock EL, Mendelsohn AD, Lo GG, Ghosh S, and O'Grady RB: Lipid keratopathy in rabbits: An animal model system. *Arch Ophthalmol* 103:726, 1985.
7. Reddy C, Stock EL, Mendelsohn AD, Nguyen HS, Roth SI, and Ghosh S: Pathogenesis of experimental lipid keratopathy: Corneal and plasma lipids. *Invest Ophthalmol Vis Sci* 28:1492, 1987.
8. Jack JL and Luce RA: Lipid keratopathy: An electron microscopic study. *Arch Ophthalmol* 83:678, 1970.
9. Karnovsky MJ: A formaldehyde-glutaraldehyde fixative of high osmolality for use in electron microscopy. *J Cell Biol* 27:137a, 1965.
10. Reynolds ES: Use of lead citrate at high pH as an electron opaque stain in electron microscopy. *J Cell Biol* 17:208, 1963.
11. Venable JH and Coggeshall RH: A simplified lead citrate stain for use in electron microscopy. *J Cell Biol* 25:407, 1965.
12. Ross R, Wight TN, Strandness E, and Thiele B: Human atherosclerosis: I. Cell constitution and characteristics of advanced lesions of the superficial femoral artery. *Am J Pathol* 114:79, 1984.
13. Brown MS and Goldstein JL: A receptor mediated pathway for cholesterol homeostasis. *Science* 232:34, 1986.
14. Basu SK, Anderson RGW, Goldstein JL, and Brown MS: Metabolism of cationized lipoproteins by human fibroblasts: Biochemical and metabolic correlations. *J Cell Biol* 74:119, 1977.
15. Stein O and Stein Y: A putative mechanism for the conversion of aortic smooth muscle cells into foam cells that bypass the autoregulatory LDL-receptor mediated process. In *Atherosclerosis VI*, Schettler G, Gotto AM, Middelhoff G, Habernicht AJR, and Jurutka KR, editors. New York, Springer Verlag, 1983, pp. 395-399.